

Original Articles

Aboveground biomass and carbon stocks in subtropical forests



Hiago Adamosky Machado ^a, Adriane Avelhaneda Mallmann ^a, Kauana Engel ^a, José Augusto Spiazzi Favarin ^a, Jordan Luis Campos Modesto ^a, Carlos Roberto Sanquetta ^a, Ana Paula Dalla Corte ^a, Henrique Soares Koehler ^a, Sylvio Péllico Netto ^a, Alexandre Behling ^a, Jonathan William Trautenmüller ^{b,*}

^a Federal University of Paraná, Department of Forest Science, Curitiba, Paraná 80210-170, Brazil

^b "Luiz de Queiroz" College of Agriculture (ESALQ), University of São Paulo (USP), Department of Forest Science, São Paulo 13418-900, Brazil

ARTICLE INFO

Keywords:
Ecological indicator
Multivariate adjustment
WNSUR
Climate change
Variance structure
Weighting

ABSTRACT

Quantifying plant biomass in native forests is essential to understanding ecosystem health, primary productivity, biodiversity, and the carbon cycle, contributing to climate regulation. Therefore, the objective of this study was to establish biomass estimators and quantify biomass and carbon stocks in subtropical forests in Brazil. The study area can be considered one of the largest preserved areas of the Atlantic Forest biome, covering approximately 6,000 km². Two procedures were used to quantify biomass and carbon: i) for trees with less than 50 cm of dbh, equations were established using allometric data collected; ii) for trees with more than 50 cm of dbh, the equations established by Trautenmüller et al. (2021) were used. These equations were biologically consistent and were corrected for heteroscedasticity, using the WNSUR procedure. These equations were later used to estimate the biomass of everyone in an inventory of subtropical forests in the state of Paraná, Brazil. A total of 456,302.00 ha of area with vegetation cover were found, with an average biomass stock of 117.26 Mg·ha⁻¹. The total biomass stock for the entire area was 53,505.97 Gg, and the carbon equivalent was 92,208.63 Gg, highlighting the need to preserve this area with vegetation cover. One of the most immediate actions to mitigate the effects of climate change is to reduce deforestation, which can be the result of human activities or caused by mass movement. New studies should be carried out to assess the effects of climate extremes on carbon stocks and how these can affect the lives involved.

1. Introduction

Native forests are a vital source of natural resources, among which plant biomass stands out. Quantifying biomass is essential, as it serves as an important ecological indicator that reflects the health and dynamics of ecosystems (Di Corpo and Vannini, 2014; Ma et al., 2017; Andrade et al. 2020; Maschler et al., 2022; Jiang et al., 2022; Trautenmüller et al., 2023). Biomass provides valuable information on primary productivity, resource availability, biodiversity, and ecological stability. Furthermore, it plays a central role in the carbon cycle by storing atmospheric carbon and thus contributing to climate regulation (Erb et al., 2017; Daioglou et al., 2019; Zhou et al., 2020).

To quantify forest biomass, it is common to evaluate the different

parts of trees, such as stem, branches, leaves, bark and roots, which together make up the total biomass (Behling et al., 2018; Trautenmüller et al., 2021). Measuring biomass, however, is considerably more complex when compared to variables such as tree diameter or height. For this reason, empirical models that estimate biomass based on traditional forest mensuration variables (diameter and height) are of great value to biometrists (Trautenmüller et al., 2021). These models offer greater practicality and simplicity in estimating biomass, especially when referring to specific parts of the tree (Zhao et al., 2019). However, since biomass is composed of several correlated parts, it is essential that the model used considers this correlation and variation between the parts.

Estimating biomass through allometric models stands out as an important alternative for understanding ecosystem dynamics, especially

* Corresponding author.

E-mail addresses: haadamosky@gmail.com (H.A. Machado), mallmannadriane@gmail.com (A.A. Mallmann), kauanaeg@gmail.com (K. Engel), jasflorest@yahoo.com.br (J.A.S. Favarin), jordan.cmmodesto@gmail.com (J.L.C. Modesto), carlossanquetta@gmail.com (C.R. Sanquetta), anapaulacorte@gmail.com (A.P. Dalla Corte), koehler@ufpr.br (H.S. Koehler), sylviopelelconetto@gmail.com (S. Péllico Netto), alexandre.behling@yahoo.com.br (A. Behling), jwtraute@gmail.com (J.W. Trautenmüller).

when seeking to aggregate information to ecological indicators and multiple diversity metrics (Barreto et al., 2023). By considering biomass allocation and accumulation as part of the energy dynamics in an ecosystem, these allometric models can be applied more broadly, redefining their results to aid ecological interpretations. However, the accuracy of these regression models is often limited, which represents a significant challenge for their application (Chave et al., 2014; Trautenmüller et al., 2021; David et al., 2022; Trautenmüller et al., 2023).

The use of models that ensure biological consistency is essential to achieve the property of additivity of the tree parts, so that the sum of these parts is equal to the total estimated tree biomass. A model is considered biologically consistent when it integrates these variations so that the sum of the estimates does not differ from the total biomass value (Behling et al., 2018; Sanquetta et al., 2015; Trautenmüller et al., 2021).

Another crucial aspect in biomass modeling is the use of contemporaneous correlation between tree parts, a practice reported since the 1970s as essential for multivariate adjustments. This approach allows estimating the parameters of structured models more efficiently, resulting in lower variance. Significant examples of this practice can be found in the works of Kozak (1970), Jacobs and Cunia (1980), Chiyenda and Kozak (1984), Reed and Green (1985), Affleck and Diéguez-Aranda (2016), Behling et al. (2018), Trautenmüller et al. (2021), and Parresol (1999, 2001). More consistent estimators increase the confidence in using tree biomass as an ecological indicator.

At a time when discussions about the possible effects and impacts of climate change on society and nature are on the rise (IPCC - Climate Change, 2021). Using good ecological indicators is essential to better understand the occurrence and dynamics of these changes. Climate change caused by global warming is increasing the intensity and frequency of natural disasters (Tradowsky et al., 2023; Tao et al., 2023). Large-scale climate events that should occur every century (Ferreira, 2024) have increased in frequency since the beginning of the century (Tao et al., 2023).

Extreme climatic events such as storms and high rainfall levels aggravate the occurrence of disasters in areas with mountainous terrain, which is characteristic of the main preserved areas of the Atlantic Forest biome in Brazil. The Atlantic Forest biome is one of the most important phytophysiognomies on the planet due to its high number of endemic species (Myers et al., 2000) and threatened with extinction. There are few large preserved areas, the largest of which are located in the coastal regions of the southern and southeastern states of Brazil. These areas have extremely rugged terrain, which makes human intervention difficult. However, they have large stocks of forest biomass and high biodiversity.

This raises some questions: i) What is the importance of forest biomass as an ecological indicator? ii) What are the biomass and carbon stocks in these conserved areas? iii) Can possible natural disasters result in biomass loss and this carbon emitted into the atmosphere?

In this sense, this study hypothesizes that forest biomass is of great importance for studying areas at risk of disasters, especially when used as an ecological indicator. Thus, this study has the following objectives: i) establish more consistent biomass estimators for Subtropical Forests in Southern Brazil; ii) identify the importance of forest biomass as an ecological indicator in the study area; iii) quantify biomass and carbon stocks for the Serra do Mar in the state of Paraná – Brazil.

2. Materials and methods

2.1. Study area

The study was carried out in subtropical forests that predominate in the “Serra do Mar” mountain range in the state of Paraná (Fig. 1). In total, it covered seven municipalities, with coordinates ranging from 25°15'S to 26°00'S, 48°00'W to 49°00'W. The altitude ranges from 0 to 1,922 m above sea level, under the domain of the Dense Ombrophilous Forest (IBGE - Instituto Brasileiro de Geografia e Estatística, 2012). The

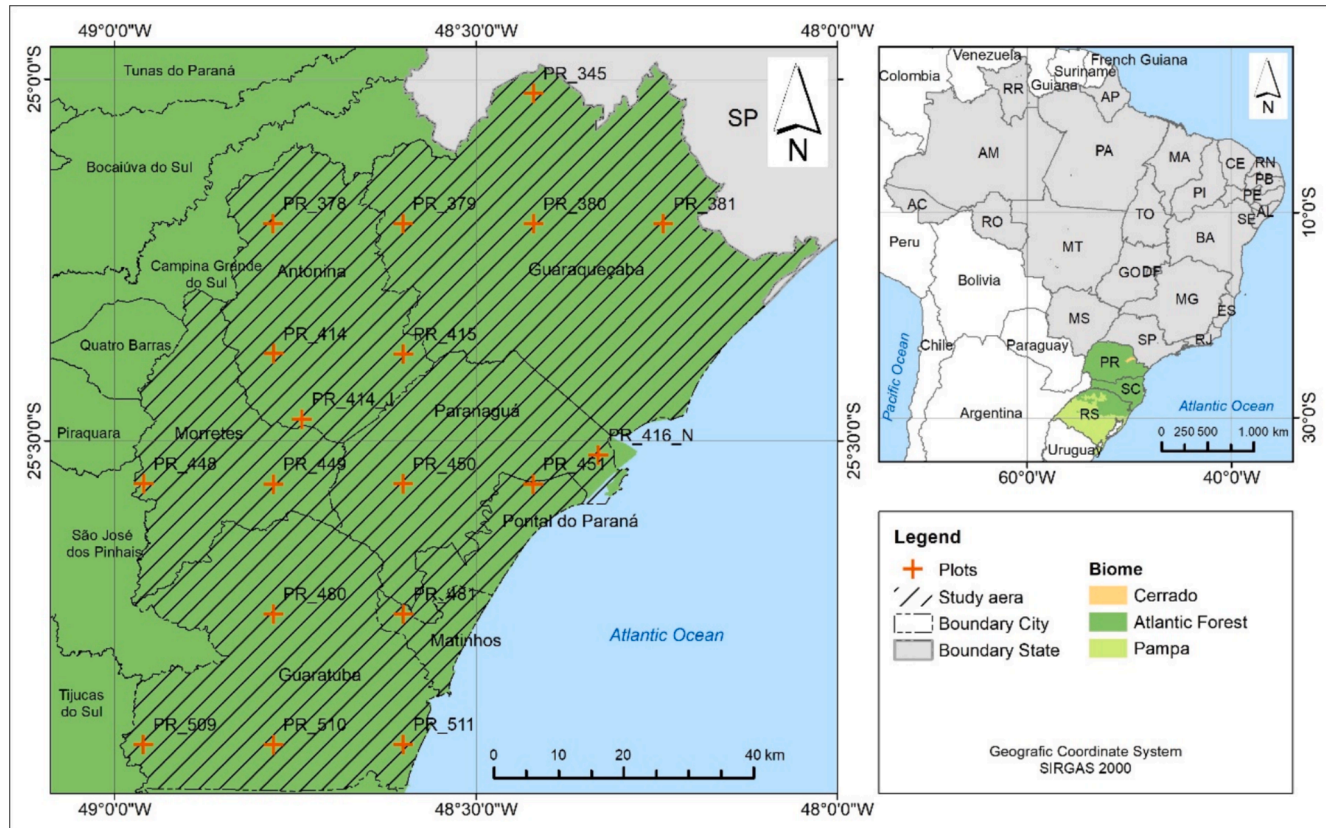


Fig. 1. Location of the study area with the sampling points of the National Forest Inventory (NFI-BR) inserted in the subtropical forest, state of Paraná – Brazil.

climate of the predominant region is classified as Cfa with a transition area to Cfb, with an average annual temperature between 16 and 22°C and average annual precipitation between 1,900 and 2,500 mm (Alvares et al., 2014).

2.2. Multivariate adjustment of biomass models

To estimate biomass, data from the National Forest Inventory (NFI-BR) (SFB - SERVIÇO FLORESTAL BRASILEIRO, 2018a) (<https://snif.forestal.gov.br/pt-br/inventario-florestal-nacional-ifn/ifn-dados-abertos/ifn-resultados-parana>) were used. These data were collected using a two-stage systematic sampling method, with the primary unit structured as a Maltese cross. Each primary unit consisted of four 20 x 50 m subplots. There is no known two-stage sampling system in the literature in which both stages are systematic. In Péllico Netto and Brena (1997), there are approximate estimators; however, the first stage is random (A appendix 1). Two approaches were applied to estimate aboveground tree biomass, as described below. A summary of the procedures used is shown in Fig. 2.

Procedure 01

Equations were generated using a database of 185 trees sampled in the state of Santa Catarina from the same forest typology. A total of 67 tree species were sampled, with the full list provided in A appendix 2. This represents approximately 10 % of the total species recorded for the Dense Ombrophilous Forest by the NFI-SC (SFB - SERVIÇO FLORESTAL BRASILEIRO, 2018b), including trees, palms, and ferns. These trees were less than 50 cm in diameter at 1.30 m aboveground (dbh). All felled individuals were evaluated for the following variables: dbh, measured using a tape measure, and total height (h), measured using a tape measure, both with precision of one millimeter.

Biomass was measured for the stem parts (wood from the stem with bark), branches and leaves, using the definitions of Picard et al. (2012). For each tree, the parts were separated and weighed using a scale to obtain the wet weight of each part. To determine the dry biomass of the parts, samples were taken immediately after weighing the wet biomass

and their masses were measured using a digital scale with a precision of 0.1 g. From the data, the dry biomass of each part was calculated, with the total biomass being the sum of the parts.

To adjust the independent biomass equations, traditional volumetric models were tested using the independent variables dbh (in cm) and h (in m). The linear models were adjusted using Ordinary Least Squares and the nonlinear models using Generalized Least Squares (Greene, 2012).

The quality of the adjustment of the equations was assessed by the Adjusted Coefficient of Determination ($R^2_{adj.}$), Coefficient of Variation, in percentage (CV%), and Akaike Information Criterion (AIC). The results of the individual performance of each model were not presented, as this was not the objective of this study.

The Schumacher and Hall (1933) and Spurr (1952) models were selected for adjustments of the stem, branches, leaves and total biomass aboveground, as defined in (01).

$$\hat{y}_{stem} = \beta_1 \bullet dbh^{\beta_2} \bullet h^{\beta_3} + \varepsilon_{stem}$$

$$\hat{y}_{branches} = \beta_1 \bullet (dbh^2 \bullet h)^{\beta_1} + \varepsilon_{branches}$$

$$\hat{y}_{leaves} = \beta_1 \bullet dbh^{\beta_2} \bullet h^{\beta_3} + \varepsilon_{leaves}$$

$$\hat{y}_{total} = \beta_1 \bullet dbh^{\beta_2} \bullet h^{\beta_3} + \varepsilon_{total}$$

(1)

The White (1980) was applied to test the hypothesis of homogeneity of the residuals in each equation with 95 % probability. For cases in which the hypothesis was rejected, weights were obtained through the variance structure (Behling et al., 2018), the application of the weights is described below (02).

$$\beta = \left(X \Psi(\hat{\theta})^{-1} X \right)^{-1} X \Psi(\hat{\theta})^{-1} y \quad (02)$$

Where: $\Psi(\hat{\theta})$ is the diagonal matrix of weights, which depends on the number of parameters (P) denoted by the vector θ of order ($P \bullet 1$).

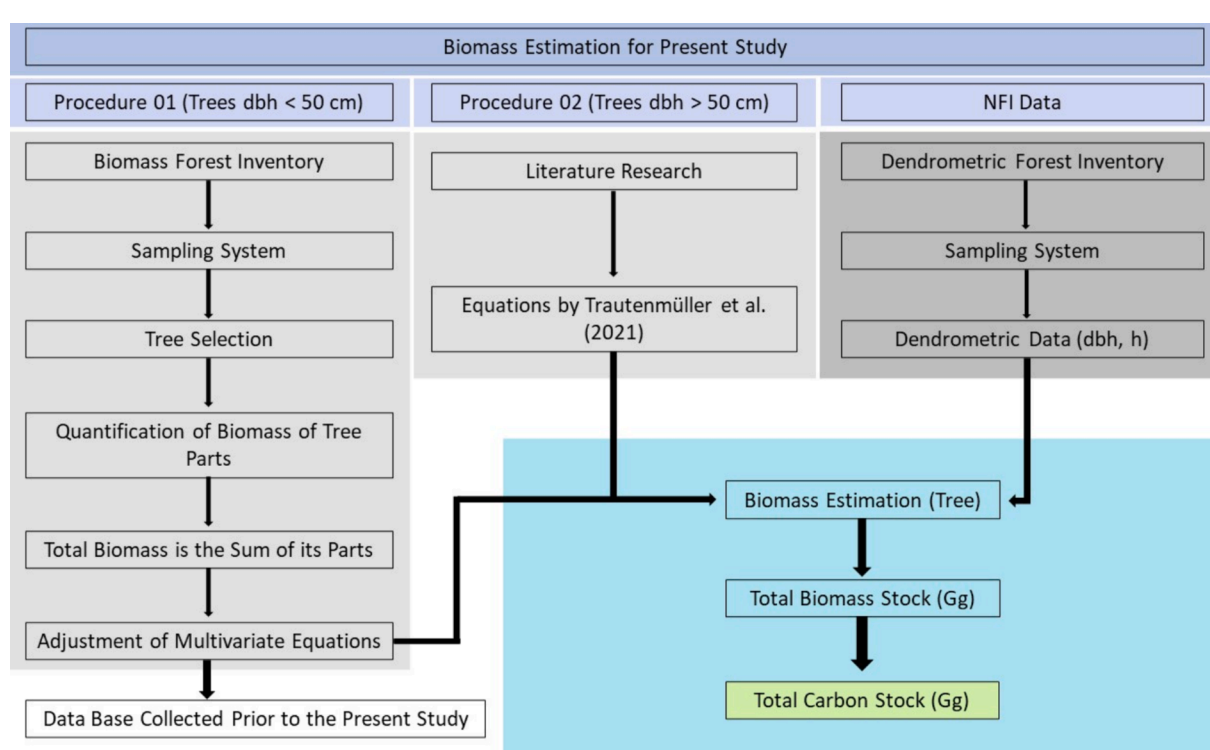


Fig. 2. Flowchart detailing the allometric procedures used to estimate the biomass of each inventoried tree, and the integration with NFI (National Forest Inventory) data to find the estimated biomass and carbon stocks for the entire study area.

The partial derivative functions referring to the matrix $f(\hat{\beta})$ and the variance-covariance matrices of $\hat{\beta}_i$ (where i refers to the coefficient of each equation) were presented, information that is useful for making inferences regarding the estimation of parameters.

To adjust the multivariate regression models for total aboveground biomass and its parts (stem, branches and leaves), the equations defined in (03) were used. For total biomass, the model considered was based on the models of each part, thus, the following system of equations was defined.

$$\begin{aligned}\hat{y}_{stem} &= \beta_{11} \bullet dbh^{\beta_{12}} \bullet h^{\beta_{13}} + \varepsilon_{stem} \\ \hat{y}_{branches} &= \beta_{21} \bullet (dbh^2 \bullet h)^{\beta_{21}} + \varepsilon_{branches} \\ \hat{y}_{leaves} &= \beta_{31} \bullet dbh^{\beta_{32}} \bullet h^{\beta_{33}} + \varepsilon_{leaves} \\ \hat{y}_{total} &= \beta_{11} \bullet dbh^{\beta_{12}} \bullet h^{\beta_{13}} + \beta_{21} \bullet (dbh^2 \bullet h)^{\beta_{21}} + \beta_{31} \bullet dbh^{\beta_{32}} \bullet h^{\beta_{33}} + \varepsilon_{total}\end{aligned}\quad (3)$$

To adjust the multivariate regression models, apparently unrelated nonlinear regression (NSUR) was used. The [White \(1980\)](#) was used to verify the hypothesis of homogeneity of the residuals in all equations (simultaneous and independent) at 95 % probability. In cases of rejection of the hypothesis, weighting was applied using weights ([Parresol, 1999, 2001; Behling et al., 2018; Trautenmüller et al., 2021](#)). Once the weights were obtained through the variance structure, the models were adjusted using apparently unrelated weighted nonlinear regression (WNSUR). The equations were evaluated by R^2 adj., CV% and AIC.

Performance tests (04) and the Chi-Square test were also used to verify whether the estimates of the two methods presented significant differences.

$$D = \frac{(\hat{I}_n - \hat{M}_n)}{\hat{I}_n} 100 \quad (4)$$

Where: D is the difference (in %) between the estimators or statistics obtained by the independent and multivariate adjustment; \hat{I}_n are the estimators or statistics obtained by the independent adjustment; \hat{M}_n are the estimators or statistics obtained by the multivariate adjustment; \hat{y}_i is the biomass estimate and $\sigma_{\hat{y}_i}^2$ is the variance for the equation i .

Procedure 02

Trees with more than 50 cm dbh were used. Thus, the equations published by [Trautenmüller et al. \(2021\)](#) were used, for the simultaneous equations in (05) to (08), which were weighted. These equations were adjusted to estimate the biomass of subtropical forests in Southern Brazil, but this sampling did not cover the present study area.

Equations.

R^2 adj. CV (%) AIC White.

$$\begin{aligned}\hat{y}_{stem} &= 0.028726 \bullet dbh^{1.675713} \bullet h^{1.165411} & 94.86 \% & 61.06 & 5,985.8 \\ 12.75 \text{ ns} & (05).\end{aligned}$$

$$\begin{aligned}\hat{y}_{branches} &= 0.003816 \bullet (dbh^2 \bullet h)^{1.121684} & 93.02 \% & 92.45 & 6,242.4 \\ 7.45 \text{ ns} & (06).\end{aligned}$$

$$\begin{aligned}\hat{y}_{leaves} &= 0.014257 \bullet (dbh^2 \bullet h)^{0.671907} & 60.46 \% & 131.79 & 4,165.9 \\ 0.64 \text{ ns} & (07).\end{aligned}$$

$$\hat{y}_{total} = \hat{y}_{stem} + \hat{y}_{branches} + \hat{y}_{leaves} \quad 97.95 \% \quad 42.75 \quad 6,226.0 \quad 19.17 \text{ ns} \quad (08).$$

Pearson correlation analysis was conducted to compare the estimates obtained from the multivariate equations developed in this study with those derived from the equations of [Trautenmüller et al. \(2021\)](#).

2.3. Forest biomass and carbon estimates

The equations to estimate aboveground biomass were applied to the NFI-BR data, whose database contains 4,170 trees evaluated for dbh and h. This database consists of 18 sampling units with 4000 m^2 each,

totaling a sampled area per inventory of 7.2 ha. The inventory system was systematic in quadrants of $20 \times 20 \text{ km}$, two sampling units were relocated, since the predicted coordinate is located at sea. Each sampling unit was allocated in the shape of a Maltese cross ([SFB - SERVIÇO FLORESTAL BRASILEIRO, 2018a](#)), with four subsamples. The sampling intensity of the inventory was 0.00002 %.

After calculating individual biomass in each plot, the average biomass stock per hectare was estimated. All calculations were performed using the software SAS OnDemand for Academics ([SAS Institute Inc., 2012](#)) and ([R Core Team, 2024](#)).

The biomass per hectare was multiplied by the total study area to estimate the total aboveground biomass within the area of interest. The total aboveground carbon (C) was calculated by multiplying the biomass by the standardized factor of 0.47, as recommended by the Intergovernmental Panel on Climate Change ([IPCC – Intergovernmental Panel on Climate Change, 2006](#)). Carbon equivalent (CO_2e) was calculated by multiplying the total carbon by the conversion factor (44/12).

2.4. Forest biomass: Ecological indicator

To use forest biomass as an ecological indicator, two indices are proposed, named $Index_1$ and $Index_2$.

The first is the ratio between the biomass stored in the largest trees ($\text{dbh} \geq 40 \text{ cm}$) (K) and the total biomass (T) estimated from the trees sampled in the forest inventory, as shown in equation (09).

$$Index_1 = \frac{K}{T} \quad (9)$$

[Péllico Netto et al. \(2015\)](#) developed a new index to assess the importance of species in a climax-stage Seasonal Semideciduous Forest located in Cássia, MG, Brazil, and preliminarily introduced what they called the Species Hierarchy Index (SHI) through the Relationship (\bar{g}_i/\bar{g}), where (\bar{g}_i) is the average cross-sectional area of each species and (\bar{g}) is the average cross-sectional area of the entire tree population of the stand. They also observed that the average diameter for this condition is approximately 20 cm. In this way, trees with $\text{dbh} \geq 40 \text{ cm}$ result in an SHI value of approximately ≥ 2 , which ensures that species with this condition achieve biomass values positioned in the upper-intermediate stratum of the biocenosis, with a concrete possibility of ascending to the upper stratum of the forest. This stratum is dominant and hosts the group of species with the greatest importance in the biocenosis, experiencing minimal competition for light.

[Pan et al. 2013](#) stated that the expected carbon stocks in intact forests reflect the forest structure. Therefore, the $Index_1$ will provide access to the hierarchical evolutionary degree of this structure. The higher value of this index indicates a more advanced ecological evolution of the forest structure.

The second index is the ratio between the estimated biomass stock per hectare (B) and the average potential biomass (L) for subtropical forests with similar structures, as shown in equation (10).

$$Index_2 = \frac{B}{L} \quad (10)$$

As a reference, we use the estimates provided by [Balbinot et al. \(2017\)](#). This index evaluates the forest's potential as a greenhouse gas sink, helping to mitigate the effects of climate change. A higher value of this index indicates greater potential for biomass and carbon stock.

3. Results

3.1. Multivariate adjustment of biomass models

The equations adjusted using the independent procedure and the adjustment statistics are presented in (11) to (14). The equations adjusted using the multivariate procedure are presented in (15) to (18).

| Equations | R ² adj | CV (%) | AIC | White | |
|--|--------------------|--------|----------|--------|------|
| $\hat{y}_{stem} = 0.026651 \cdot dbh^{1.756756} \cdot h^{1.098748}$ | 85.93% | 34.94 | 2,624.18 | 49.9* | (11) |
| $\hat{y}_{branches} = 0.003589 \cdot (dbh^2 \cdot h)^{1.134702}$ | 77.97% | 54.70 | 2,716.96 | 47.2* | (12) |
| $\hat{y}_{leaves} = 0.000472 \cdot dbh^{2.287631} \cdot h^{1.133934}$ | 65.57% | 70.75 | 2,120.47 | 105.5* | (13) |
| $\hat{y}_{total} = 0.024169 \cdot dbh^{2.03414} \cdot h^{1.040367}$ | 91.16% | 29.21 | 2,796.98 | 49.8* | (14) |
| $\hat{y}_{stem} = 0.028152 \cdot dbh^{1.759321} \cdot h^{1.076449}$ | 86.05% | 34.95 | 2,624.22 | 49.4* | (15) |
| $\hat{y}_{branches} = 0.003566 \cdot (dbh^2 \cdot h)^{1.135374}$ | 78.09% | 54.70 | 2,716.96 | 47.1* | (16) |
| $\hat{y}_{leaves} = 0.000398 \cdot dbh^{2.242152} \cdot h^{1.249418}$ | 65.79% | 70.82 | 2,120.85 | 101.3* | (17) |
| $\hat{y}_{total} = \hat{y}_{stem} + \hat{y}_{branches} + \hat{y}_{leaves}$ | 91.07% | 29.27 | 2,797.77 | 57.4* | (18) |

The null hypothesis for the homogeneity of the distribution of residues was verified by the White test. The test revealed that the tested hypothesis was rejected, since the alpha value corresponding to the White statistic was less than 5% probability, for all parts and the total biomass.

When fitted equations present heterogeneous residuals, there are two main approaches to achieve homogeneous residuals: data transformation or equation weighting (Carroll and Ruppert, 1988). An effective way to apply weighting is through variance structure modeling, as described by Harvey (1976). Several researchers recommend this approach (Parresol, 1999, 2001; Behling et al., 2018; Wang et al., 2018; Trautenmüller et al., 2021) to correct heteroscedasticity in biomass data. For the weighted adjustment, weights for the biomass of the parts

and for the total aboveground biomass were obtained through the variance structure, as shown in equations (19) to (22).

| Parts | Weights |
|----------------------|--|
| \hat{y}_{stem} | $\hat{\sigma}^2 = dbh^{4.251607} \cdot h^{1.045364}$ |
| $\hat{y}_{branches}$ | $\hat{\sigma}^2 = (dbh^2 \cdot h)^{1.738346}$ |
| \hat{y}_{leaves} | $\hat{\sigma}^2 = dbh^{4.610687} \cdot h^{0.583014}$ |
| \hat{y}_{total} | $\hat{\sigma}^2 = dbh^{4.796349} \cdot h^{0.70327}$ |

The results obtained with the weighting for the independent equations are presented in (23) to (26) and for the simultaneous equations they are presented in (27) to (30), all with their corresponding statistics.

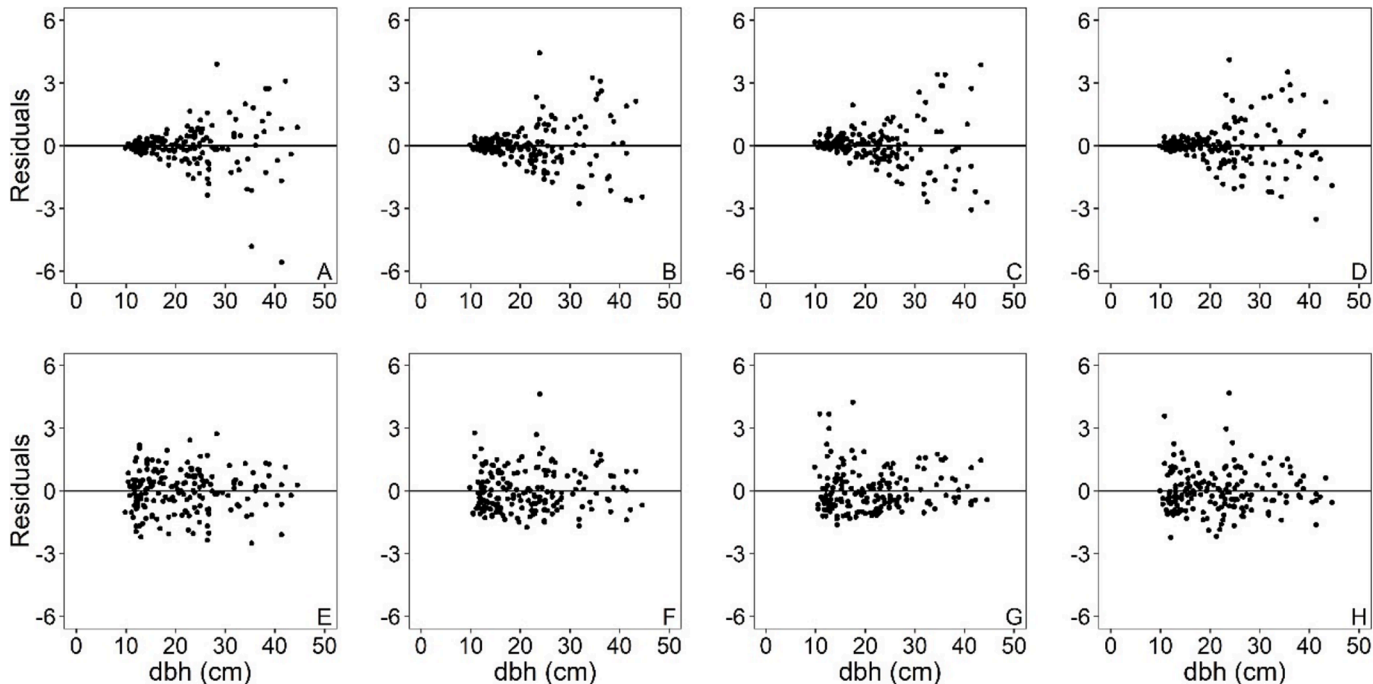


Fig. 3. Distribution of standardized residuals through independent adjustment, unweighted (first row) and weighted (second row), as a function of diameter at 1.30 m aboveground (dbh), for estimates of parts stem (A and E), branches (B and F), leaves (C and G) and total aboveground biomass (D and H).

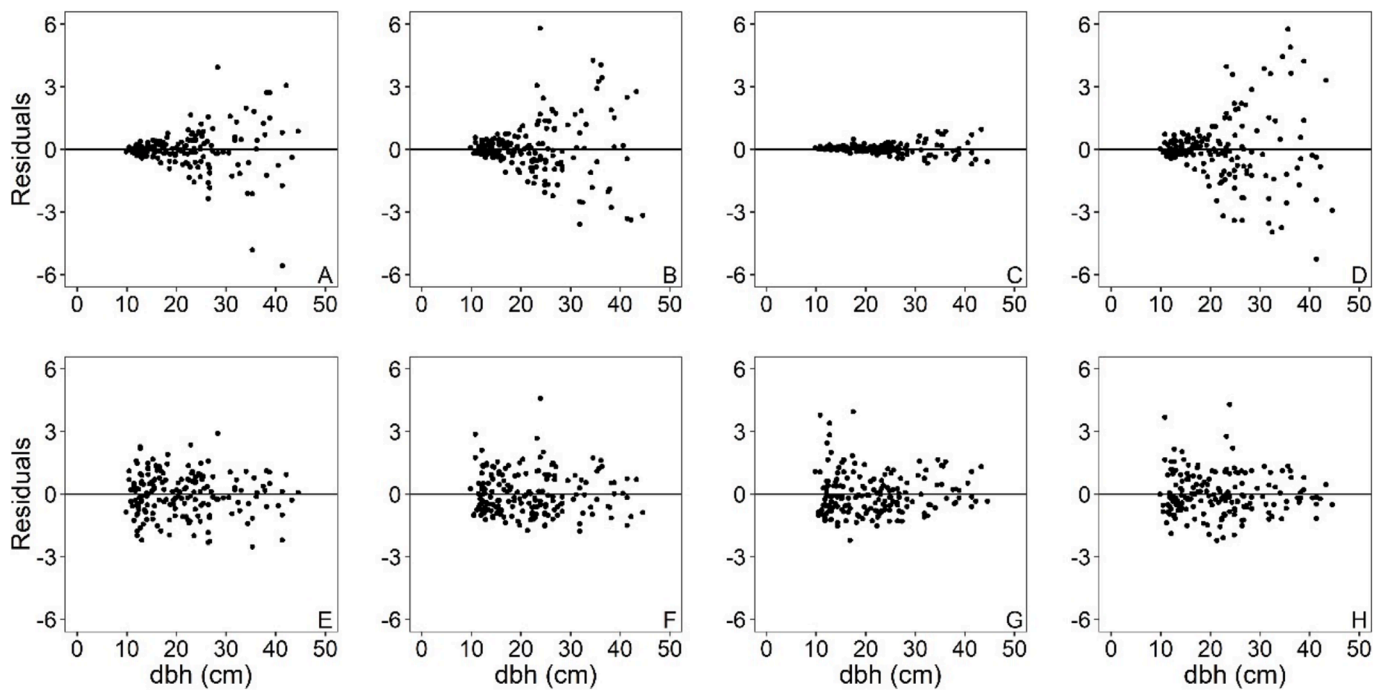


Fig. 4. Distribution of standardized residuals through multivariate adjustment, unweighted (first row) and weighted (second row), as a function of diameter at 1.30 m aboveground (dbh), for estimates of parts stem (A and E), branches (B and F), leaves (C and G) and total aboveground biomass (D and H).

| Equations | R2adj | CV (%) | AIC | White | |
|--|--------|--------|----------|--------|------|
| $\hat{y}_{stem} = 0.018761 \cdot dbh^{1.748948} \cdot h^{1.234618}$ | 85.79% | 35.13 | 2,626.03 | 1.8ns | (23) |
| $\hat{y}_{branches} = 0.007292 \cdot (dbh^2 \cdot h)^{1.060027}$ | 77.62% | 55.14 | 2,719.74 | 6.3ns | (24) |
| $\hat{y}_{leaves} = 0.011097 \cdot dbh^{2.029614} \cdot h^{0.300514}$ | 60.60% | 75.68 | 2,144.33 | 9.4ns | (25) |
| $\hat{y}_{total} = 0.046233 \cdot dbh^{2.121703} \cdot h^{0.702375}$ | 90.37% | 30.49 | 2,812.23 | 6.8ns | (26) |
| $\hat{y}_{stem} = 0.022785 \cdot dbh^{1.872289} \cdot h^{1.019728}$ | 85.80% | 35.26 | 2,627.40 | 1.7ns | (27) |
| $\hat{y}_{branches} = 0.003992 \cdot (dbh^2 \cdot h)^{1.120316}$ | 77.89% | 54.95 | 2,718.58 | 7.0ns | (28) |
| $\hat{y}_{leaves} = 0.002957 \cdot dbh^{1.754425} \cdot h^{1.107952}$ | 62.59% | 74.06 | 2,136.65 | 15.4ns | (29) |
| $\hat{y}_{total} = \hat{y}_{stem} + \hat{y}_{branches} + \hat{y}_{leaves}$ | 91.08% | 29.26 | 2,797.60 | 17.3ns | (30) |

The weights established by the variance structure modeling allowed for the homoscedasticity of the residuals, as demonstrated by the White test and the graphical analysis of the residuals (Fig. 3 and Fig. 4). Thus, it was possible to find true confidence intervals. All coefficients were significant at 95 % probability with the application of the *t*-test.

The variance–covariance matrices of $\hat{\beta}_i$, where i are the coefficients of each equation, for the independent fit are presented in (31) to (34) and for the multivariate fit in (35).

$$\hat{\Sigma}_{\beta_{y_{stem}}} = \begin{array}{c|ccc} & \hat{\beta}_1 & \hat{\beta}_2 & \hat{\beta}_3 \\ \hat{\beta}_1 & 0.0000153 & -0.0000406 & -0.0002580 \\ \hat{\beta}_2 & -0.0000406 & 0.0042409 & -0.0039338 \\ \hat{\beta}_3 & -0.0002580 & -0.0039338 & 0.0095815 \end{array} \quad (31)$$

$$\hat{\Sigma}_{\beta_{y_{branches}}} = \begin{array}{c|cc} & \hat{\beta}_1 & \hat{\beta}_2 \\ \hat{\beta}_1 & 0.0000071 & -0.0001074 \\ \hat{\beta}_2 & -0.0001074 & 0.0016456 \end{array} \quad (32)$$

$$\hat{\Sigma}_{\beta_{y_{leaves}}} = \begin{array}{c|ccc} & \hat{\beta}_1 & \hat{\beta}_2 & \hat{\beta}_3 \\ \hat{\beta}_1 & 0.0000285 & -0.0001292 & -0.0008402 \\ \hat{\beta}_2 & -0.0001292 & 0.0246388 & -0.0233696 \\ \hat{\beta}_3 & -0.0008402 & -0.0233696 & 0.0557980 \end{array} \quad (33)$$

$$\hat{\Sigma}_{\beta_{y_{total}}} = \begin{array}{c|ccc} & \hat{\beta}_1 & \hat{\beta}_2 & \hat{\beta}_3 \\ \hat{\beta}_1 & 0.0000830 & -0.0000869 & -0.0005801 \\ \hat{\beta}_2 & -0.0000869 & 0.0039283 & -0.0037169 \\ \hat{\beta}_3 & -0.0005801 & -0.0037169 & 0.0089800 \end{array} \quad (34)$$

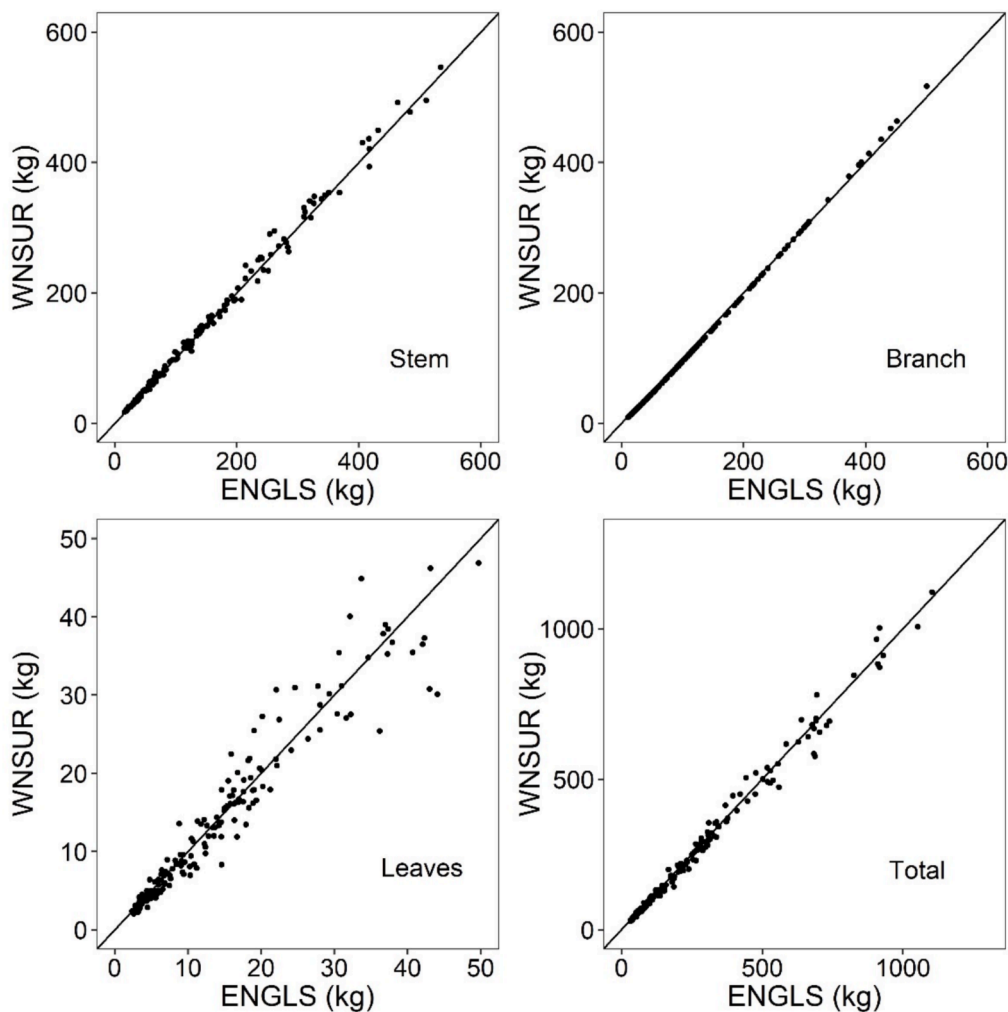


Fig. 5. Relationship between biomass values estimated through independent adjustment (ENGLS) and biomass estimated through multivariate adjustment (WNSUR) for parts and total aboveground biomass in subtropical forests in Brazil.

$$\begin{aligned}
 \hat{\Sigma}_{\beta_y} &= \begin{array}{cccccccc} \hat{\beta}_{11} & \hat{\beta}_{12} & \hat{\beta}_{13} & \hat{\beta}_{21} & \hat{\beta}_{22} & \hat{\beta}_{31} & \hat{\beta}_{32} & \hat{\beta}_{33} \end{array} \\
 &= \begin{array}{|c c c c c c c c c|} \hline
 \hat{\beta}_{11} & 0.0000219 & -0.0000622 & -0.0002895 & -0.0000012 & 0.0000321 & -0.0000001 & 0.0000390 & -0.0000317 \\
 \hat{\beta}_{12} & -0.0000622 & 0.0039100 & -0.0033716 & 0.0000239 & -0.0006647 & 0.0000106 & -0.00003921 & -0.0009121 \\
 \hat{\beta}_{13} & -0.0002895 & -0.0033716 & 0.0086034 & -0.0000087 & 0.0002387 & -0.0000103 & -0.0002379 & 0.0015905 \\
 \hat{\beta}_{21} & -0.0000012 & 0.0000239 & -0.0000087 & 0.0000011 & -0.0000289 & 0.0000005 & -0.0000330 & -0.0000187 \\
 \hat{\beta}_{22} & 0.0000321 & -0.0006647 & 0.0002387 & -0.0000289 & 0.0007952 & -0.0000128 & 0.0008781 & 0.0005507 \\
 \hat{\beta}_{31} & -0.0000001 & 0.0000106 & -0.0000103 & 0.0000005 & -0.0000128 & 0.0000016 & -0.0000393 & -0.0001571 \\
 \hat{\beta}_{32} & 0.0000390 & -0.0003921 & -0.0002379 & -0.0000330 & 0.0008781 & -0.0000393 & 0.0170337 & -0.0141020 \\
 \hat{\beta}_{33} & -0.0000317 & -0.0009121 & 0.0015905 & -0.0000187 & 0.0005507 & -0.0001571 & -0.0141020 & 0.0356868 \\
 \hline
 \end{array} \quad (35)
 \end{aligned}$$

The variance-covariance matrix of the residuals for the simultaneously fitted equations is presented in (36).

$$\hat{\sigma}_{ij} = \begin{array}{|c c c c|} \hline
 y_{stem} & y_{branches} & y_{leaves} & y_{total} \\
 \hline
 y_{stem} & 0.0001073 & -0.0000306 & -0.0000017 & 0.0000556 \\
 y_{branches} & -0.0000306 & 0.0003890 & 0.0000362 & 0.0002117 \\
 y_{leaves} & -0.0000017 & 0.0000362 & 0.0000100 & 0.0000263 \\
 y_{total} & 0.0000556 & 0.0002117 & 0.0000263 & 0.0001731 \\
 \hline
 \end{array} \quad (36)$$

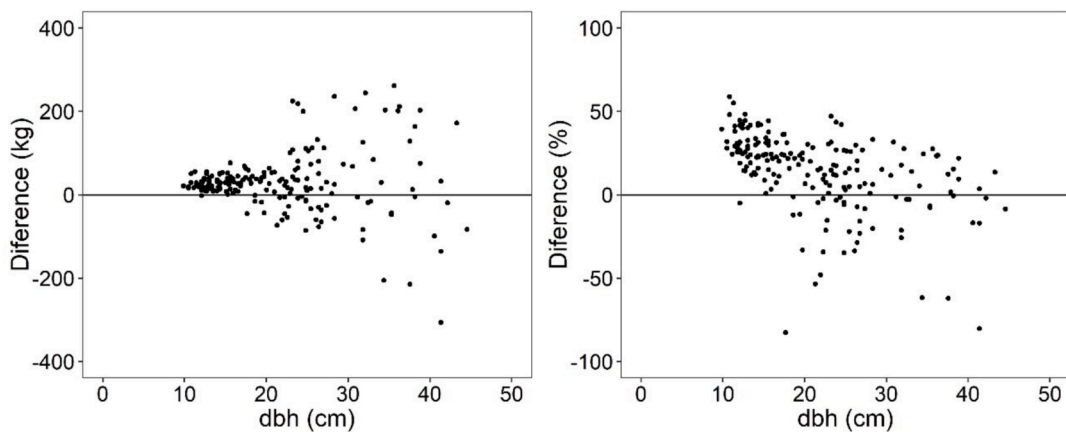


Fig. 6. Non-additivity of total aboveground biomass estimated by independent adjustment as a function of diameter at 1.3 m aboveground (dbh) in trees from subtropical forests in Brazil.

3.2. Comparison of independent and multivariate adjustments

The independent and multivariate adjusted equations showed similar performance trends even with differences in the coefficients. The multivariate adjustment is the only method that ensures the additivity of estimates for tree components, making it the approach used for biomass estimation in this study. For the stem, branches and leaves parts, the

greatest differences were observed for the scale coefficient of the equations ($\hat{\beta}_3$ e $\hat{\beta}_{x3}$), which varied between -268.69 and 17.41% , respectively, while the other coefficients varied from -21.45 to 73.35% . For the precision statistics, the leaves part presented the greatest differences for $R^2_{adj.}$, CV and AIC, which were -0.34 , -0.10 and -0.02% , respectively. For the stem and branches parts, all precision statistics varied from -0.15 to 0.01% .

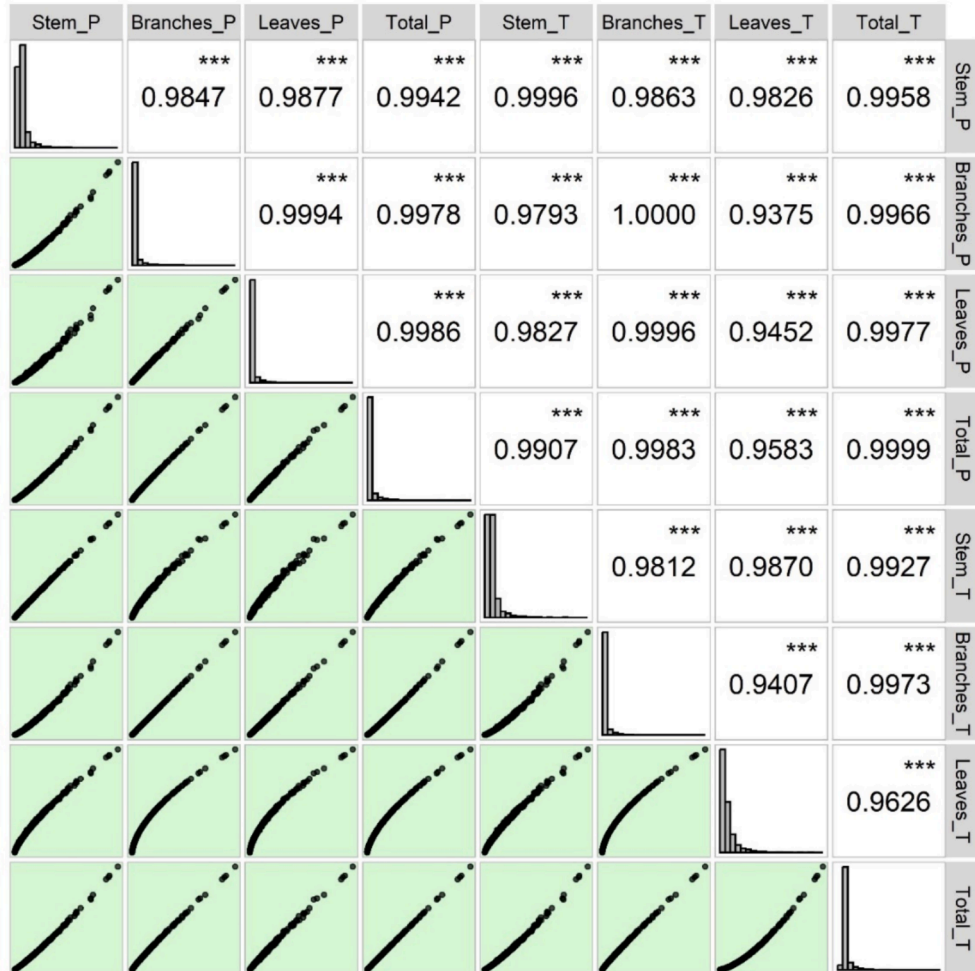


Fig. 7. Correlations between the estimates of the multivariate equations found in the present study (part_P) with the estimates of the equations published by Trautenmüller et al. (2021) (part_T).

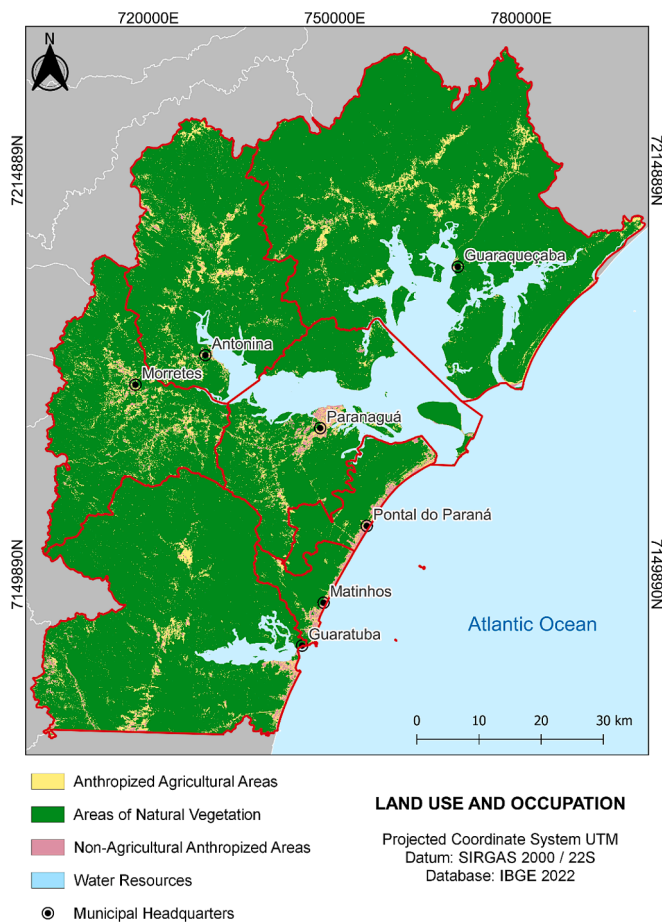


Fig. 8. Land use in the Serra do Mar, coastal region of the state of Paraná – BR, image of the year 2022.

Table 1

Stocks of biomass, carbon and Carbon equivalent (CO_2e) in Serra do Mar, Paraná – BR, based on land use and occupation in 2022.

| Metrics | Values(Confidence Interval) |
|--|-----------------------------|
| Total area (Km^2) | 6,055.34 |
| Vegetated area (Km^2) | 4,563.02 |
| Vegetated area (ha) | 456,302.00 |
| Biomass ($\text{Mg} \cdot \text{ha}^{-1}$) | 117.26 ± 23.36 |
| Standard error of estimate (%) | 19.16 |
| Biomass Stock (Gg) | $53,505.97 \pm 10,254.37$ |
| Carbon Stock (Gg) | $25,147.81 \pm 4,819.55$ |
| Carbon equivalent (CO_2e) stock (Gg) | 92,208.63 |

Table 2

Number of trees per hectare for the present study, number of trees larger than 40 cm in dbh (diameter at 1.30 m aboveground), biomass found by [Balbinot et al. \(2017\)](#) and the values of the indices proposed in the present work.

| Metrics | Values |
|--|-----------|
| Total tree ($\text{tree} \cdot \text{ha}^{-1}$) | 579.2 |
| Total biomass of trees (kg) | 731,348.7 |
| Tree > 40 cm of dbh ($\text{tree} \cdot \text{ha}^{-1}$) | 29.9 |
| Total biomass of trees > 40 cm of dbh (kg) | 295,391.4 |
| Tree biomass Balbinot et al. (2017) ($\text{Mg} \cdot \text{ha}^{-1}$) | 371.1 |
| Index_1 | 0.404 |
| Index_2 | 0.316 |

The relationship between the biomasses estimated through independent and multivariate adjustment are shown in [Fig. 5](#). The biomass values estimated for the stem, branches, leaves and total biomass showed a small difference between the two forms of adjustment, being considered non-significant by the Chi-square test (stem = 0.61 ns; branches = 0.01 ns; leaves = 1.49 ns; total = 10.49 ns).

Biomass estimates through independent adjustment did not result in biologically consistent values, i.e., $\hat{y}_{\text{stem}} + \hat{y}_{\text{branches}} + \hat{y}_{\text{leaves}} - \hat{y}_{\text{total}} \neq 0$. The non-additivity of the independent equations is shown in [Fig. 6](#), these differences varied between -97.54 and 49.39 %.

3.3. Comparison of multivariate equations with those of [Trautenmüller et al. \(2021\)](#)

A high correlation can be observed between the estimates ([Fig. 7](#)) of the multivariate equations (Procedure 1) and the estimates of the equations by [Trautenmüller et al. \(2021\)](#) (Procedure 2). For the stem, branches, leaves and total biomass parts the correlations between the estimates were 0.9996, 1.0000, 0.9452 and 0.9999, respectively.

3.4. Biomass and carbon stocks

The total area studied corresponds to a total of 6,055.34 km^2 , of which 4,563.02 km^2 have vegetation cover, which is equivalent to 456,302 ha (ha) ([Fig. 8](#)). The average biomass found was 120.92 $\text{Mg} \cdot \text{ha}^{-1}$ ([Table 1](#)). When applied to the total area, the accumulated biomass in the region reaches a total value of 55,176.04 Gg. Considering that 47 % of the biomass is composed of carbon, the total carbon stored in the biomass of Serra do Mar was calculated at 25,932.74 Gg. The total carbon stored corresponds to an equivalent of 95,096.22 Gg of CO_2 , reflecting the importance of this region in the retention of atmospheric carbon and its contribution to the mitigation of climate change.

3.5. Forest biomass: Ecological indicator

The NFI ([SFB - SERVIÇO FLORESTAL BRASILEIRO, 2018a](#)) data used in this study presented 4,170 trees, which represents 579.2 $\text{trees} \cdot \text{ha}^{-1}$ ([Table 2](#)). A total of 29.9 $\text{trees} \cdot \text{ha}^{-1}$ with more than 40 cm of dbh were found, these trees represent 5.16 % of the total trees found in one hectare. The value calculated for the proposed Index_1 (09) was 0.404, indicating that 40.4 % of the tree biomass is allocated to trees with a diameter at breast height (dbh) greater than 40 cm. For Index_2 (10), the value obtained was 0.316.

4. Discussion

Studies that quantify biomass stocks using allometric equations constantly face the problem of a lack of homoscedasticity for the models generated. [Cunia and Briggs \(1984\)](#) suggests that there is less variability in the biomass of smaller individuals when compared to larger ones. For this reason, heteroscedasticity of the residues was observed. As pointed out by several authors ([Parresol, 1999, 2001; Basuki et al. 2009, Bi et al. 2010; Zeng et al. 2011; Blujdea et al. 2012; Sileshi, 2014; Sanquette et al. 2015, Zhao et al. 2015, Wang et al. 2018; Oliveira et al., 2017; Behling et al., 2018; Trautenmüller et al., 2021; Trautenmüller et al., 2023](#)), heterogeneity in the distribution of residuals is frequently found. To solve this problem, the resulting models were weighted. Weighting based on the variance structure ([Behling et al., 2018; Trautenmüller et al., 2021](#)) was sufficient to correct the distribution of residuals ([Figs. 2 and 3](#)).

According to the work carried out by [Behling et al. \(2018\)](#), this

element of variation along the diameter gradient can explain the heterogeneity of the residues. Some parts may present greater variance than others, as pointed out by Trautenmüller et al. (2021), when demonstrating that the estimates of some parts, such as the biomass of leaves of native species, present greater coefficients of variation.

As Greene (2012) points out, heteroscedasticity correction should be performed whenever it is detected, as it is not an ideal factor for regression analyses. The homogeneity of the distribution of residuals is directly related to the validation of hypotheses tested in the models (Gujarati & Porter, 2009). To solve the problem of heteroscedasticity, the variance structure was used as weighting (Parresol, 1999, 2001; Balboa-Murias et al., 2006; Oliveira et al., 2017; Behling et al., 2018; Trautenmüller et al., 2021). Correction of the variation for the highest diametric values can also be observed in the graphs of the standardized residuals (Figs. 2 and 3).

The use of the variance structure in the weighting was able to reduce the variation in the dispersion of the residues for the larger diameters. Despite this correction, the weighted model began to present greater variation for the residues in the smaller diameters, thus inverting the expected relationship for the variation of the residues along the diametric gradient.

As expected, only the multivariate adjustment presents additivity between the parts, while the independent adjustment demonstrated divergent results between the estimate for the total and the sum of the estimates for parts (Fig. 6). The coefficients adjusted by the multivariate procedure presented less variation between each other. The coefficients adjusted by the independent adjustment presented greater variation between each other. These results are feasible, since the multivariate adjustment considers contemporary correlations in its procedure, thus increasing efficiency and obtaining biological consistency (Behling et al., 2018). Similar results were found by Trautenmüller et al. (2021) when studying the independent and multivariate adjustment for subtropical forests in Brazil.

As shown in Fig. 7, the correlations between the estimates from procedures 1 and 2 are highly significant. The literature continues to debate whether local or global models are better suited for estimating different forest variables (Basuki et al., 2009; Chave et al., 2014; Lima et al., 2017; Trautenmüller et al., 2021). However, tree allometry varies across species and regions of origin (Basuki et al., 2009; Timilsina et al., 2017; Trautenmüller et al., 2023), with soil and climate variables influencing these relationships across different locations.

For this reason, equations were specifically developed for the Dense Ombrophilous Forest, as this forest type was not included in the equations of Trautenmüller et al. (2021). However, the equations derived in this study for the Dense Ombrophilous Forest had a diameter limit of 50 cm at breast height (dbh). Consequently, trees sampled by the NFI with a dbh greater than 50 cm were estimated using the equations from Trautenmüller et al. (2021).

With efficient and biologically consistent equations, biomass becomes an important ecological indicator (Trautenmüller et al., 2023) of ecosystem health and dynamics (Ma et al., 2017; Andrade et al., 2020; Maschler et al., 2022; Jiang et al., 2022). This stability, quality, and dynamics can be negatively affected by climate extremes. Storms affect topographically critical regions with a greater chance of landslides (Ferreira, 2024). Under these conditions, regions with mountainous relief become highly unstable, susceptible to the occurrence of large mass movements.

The study region (Serra do Mar – Paraná) is one of the best-preserved areas of the Atlantic Forest biome in Brazil. This region has highly rugged terrain, where mass movements occur frequently. The forest under study may be highly vulnerable to climate change, particularly if disturbances become more frequent and intense due to the increase in climate extremes. In the future, such disturbances could threaten existing carbon stocks (Table 1), potentially turning the area into a source of CO₂ emissions.

An inventory carried out one month after an extreme rainfall event in

central Italy recorded 1,687 landslides in an area of 550 km² (Santangelo et al., 2023). The data from Santangelo et al. (2023) highlight the potential for degradation in the study area due to increasingly intense climate extremes, particularly excessive rainfall. The study area in the present research is approximately 11 times larger than the region analyzed by Santangelo et al. (2023), covering a total of 6,055.34 km². For comparison, the territorial size of Luxembourg is 2,586 km² (Hausemer, 2008), which represents 42.7 % of the area under study.

Therefore, the increase in the frequency of climate extremes may increase the likelihood of the entire study area becoming an emitter of greenhouse gases due to the loss of vegetation cover.

Therefore, the increased frequency of climate extremes could raise the likelihood of the entire study area becoming a greenhouse gas emitter due to the loss of vegetation cover.

The total carbon equivalent stock stored in the forest is nearly equivalent to the amount emitted by the state of Rio de Janeiro in 2015, totaling 92,689.74 Gg CO₂e (SEAS – Secretaria do Estado do Ambiente e Sustentabilidade, 2019).

The continued preservation of these areas is essential to maintaining the quality and quantity of life of flora and fauna, including human beings. One of the most immediate actions to mitigate the effects of climate change is to reduce deforestation (Griscom et al., 2009; Cook-Patton et al., 2021; Freund et al., 2024; Butler et al., 2024), which may be the result of human activities or caused by mass movements, which is the issue under study in this paper. New studies should be carried out to assess the effects of climate extremes on carbon stocks and how these may affect the lives involved.

With the values obtained for the proposed indices, it is evident that the forest under study has the potential to increase its biomass and carbon stock. The *Index₁* range between 0 and 1. For *Index₁*, lower values indicate younger forests; values near 0 suggest forests in early stages of regeneration. Conversely, values approaching 1 indicate forests nearing a climax state (Lindenmayer et al., 2012; Bordin et al., 2021), characterized by a higher proportion of large trees. In the present study, 40.4 % of the biomass is allocated to trees with a diameter at breast height (dbh) greater than 40 cm, which represent 5.44 % of the trees in the forest inventory.

Previous research highlights the critical role of large trees (dbh > 50 cm) in biomass allocation, with studies showing that they can account for more than 50 % of tree biomass (Goodman et al., 2014; Lutz et al., 2018; Romero et al., 2022). This suggests that the forest under study has significant potential for continued biomass accumulation. However, large trees are particularly sensitive to climate change, as noted by Lindenmayer et al. (2012) and Lutz et al. (2018). Therefore, management and conservation strategies should prioritize the preservation of these large trees.

Index₂ provides insights into the forest's biomass stock potential. Values closer to 0 indicate a forest with low biomass stocks, while values closer to 1, or even above the reference, indicate the forest's capacity to store biomass and carbon. Conversely, values near 1 suggest a maximum capacity for biomass stock, indicating a forest close to its dynamic equilibrium of growth and mortality. For the forest under study, the biomass stock was calculated at 117.26 Mg.ha⁻¹, representing 31.6 % of the stock found by Balbinot et al. (2017) in subtropical forests in Brazil. Their study reported an average biomass stock of 371.1 Mg.ha⁻¹. Similarly, Pan et al. (2013) reported an average carbon stock of 163.9 Mg.ha⁻¹ for intact tropical forests, which, when converted using a carbon content factor of 0.47 (IPCC – Intergovernmental Panel on Climate Change, 2006), corresponds to an average biomass stock of 348.72 Mg.ha⁻¹ closely aligned with the findings of Balbinot et al. (2017).

Future studies are recommended to further evaluate and validate the proposed indices. Additionally, research should examine the effects of climate extremes on carbon stocks and how these impacts can affect ecosystems and human livelihoods.

5. Conclusions

The equations obtained through the weighted multivariate procedure provide biological consistency and correction for heteroscedasticity, in addition to presenting coefficients with less variation between the parts.

The biomass and carbon stocks are important for assessing the ecological conditions of subtropical forests. The stocks found are relevant when it comes to in climate change, mainly due to the stocks found. The intensification of climate extremes caused by climate change could make the area a potential source of CO₂ emissions.

The present tropical forest has a stock of 55,176.04 Gg of tree biomass aboveground and 92,209.65 Gg of carbon equivalent stored in the aerial part of the vegetation of the studied forest.

The two indices proposed here can be considered ecological indicators based on the tree biomass of forests. *Index₁* provides information on biomass allocation and forest structure, while *Index₂* reflects the forest's potential to stock biomass or indicates whether it has reached the climax stage.

CRediT authorship contribution statement

Hiago Adamosky Machado: Writing – original draft, Software, Methodology, Investigation, Formal analysis, Data curation, Conceptualization. **Adriane Avelhaneda Mallmann:** Validation, Methodology, Formal analysis. **Kauana Engel:** Validation, Methodology, Formal analysis. **José Augusto Spiazzi Favarin:** Validation, Methodology, Formal analysis. **Jordan Luis Campos Modesto Pereira:** Methodology,

Formal analysis. **Carlos Roberto Sanquetta:** Visualization, Resources, Investigation, Funding acquisition. **Ana Paula Dalla Corte:** Visualization, Resources, Funding acquisition. **Henrique Soares Koehler:** Writing – review & editing, Validation, Methodology, Formal analysis, Data curation, Conceptualization. **Sylvio Péllico Netto:** Writing – review & editing, Validation, Methodology, Formal analysis, Conceptualization. **Alexandre Behling:** Writing – review & editing, Validation, Methodology, Formal analysis, Conceptualization. **Jonathan William Trautenmüller:** Validation, Software, Resources, Methodology, Formal analysis, Data curation, Conceptualization.

Declaration of competing interest

The authors declare that they have no known competing financial interests or personal relationships that could have appeared to influence the work reported in this paper.

Acknowledgements

This study was funded by grants from the National Council of Technological and Scientific Development (CNPq; number: 406718/2022-9; number 309824/2023-0) and the Foundation for the Support of Research of the State São Paulo (FAPESP; number: 2024/14326-0).

This study was financed in part by the Coordination for the Improvement of Higher Education Personnel - Brazil (CAPES) - Finance Code 001.

The authors would also like to thank two anonymous reviewers who made significant comments and suggestions to improve this work.

Appendix 1

Equations taken from [Péllico Netto and Brena \(1997\)](#), remembering that these authors considered the first stage random and the second systematic. In the present work, both stages were systematic. However, this approximation will be very close to the real values of the estimates with the two systematic stages.

The following are the equations:

Where:

X_{ij} is the value found in each subplot within each conglomerate;

N is the potential conglomerate number;

n is the number of conglomerate sampled;

M is the number of subplots within the conglomerate;

t is the tabulated value of the Student's t distribution.

- Mean within each conglomerate:

$$\bar{x}_i = \frac{\sum_{j=1}^M X_{ij}}{M}$$

- Mean between conglomerates:

$$\bar{x} = \frac{\sum_{i=1}^n \sum_{j=1}^M X_{ij}}{nM}$$

- Variance within conglomerates:

$$s_d^2 = \frac{\sum_{i=1}^n \sum_{j=1}^M (X_{ij} - \bar{x}_i)^2}{n(M-1)}$$

- Variance between conglomerates:

$$s_e^2 = \frac{\left(\frac{\sum_{i=1}^n M \cdot (\bar{x}_i - \bar{x})^2}{n-1} \right) - s_d^2}{M}$$

- Standard error of mean:

$$s_{\bar{x}} = \sqrt{\left(\frac{N-n}{N}\right) \cdot \frac{s_e^2}{n} + \frac{s_d^2}{n \cdot M}}$$

- Standard error of estimate:

$$E_r = \pm \left(\frac{t \cdot s_{\bar{x}}}{\bar{x}} \right) * 100$$

- Confidence interval for the mean, 95 % confidence:

$$IC[\bar{x} - t \cdot s_{\bar{x}} \leq \bar{X} \leq \bar{x} + t \cdot s_{\bar{x}}] = P$$

- Confidence interval for total area, 95 % confidence:

$$IC[\bar{x} - N \cdot M \cdot t \cdot s_{\bar{x}} \leq \bar{X} \leq \bar{x} + N \cdot M \cdot t \cdot s_{\bar{x}}] = P$$

Table A2

List of species sampled in the biomass collection for trees with up to 50 dbh, in Santa Catarina, column No. represents the number of trees sampled for each species.

| List | Scientific name | Family | No. |
|------|-----------------------------------|-----------------|-----|
| 1 | <i>Prunus myrtifolia</i> | Rosaceae | 2 |
| 2 | <i>Posoqueria latifolia</i> | Rubiaceae | 2 |
| 3 | <i>Casearia sylvestris</i> | Flacourtiaceae | 3 |
| 4 | <i>Tabebuia cassinooides</i> | Bignoniaceae | 3 |
| 5 | <i>Matayba elaeagnoides</i> | Sapindaceae | 6 |
| 6 | <i>Cupania vernalis</i> | Sapindaceae | 1 |
| 7 | <i>Nectandra lanceolata</i> | Lauraceae | 3 |
| 8 | <i>Ocotea catharinensis</i> | Lauraceae | 2 |
| 9 | <i>Ocotea nectandrifolia</i> | Lauraceae | 7 |
| 11 | <i>Cryptocarya aschersoniana</i> | Lauraceae | 3 |
| 12 | <i>Endlicheria paniculata</i> | Lauraceae | 3 |
| 13 | <i>Ocotea puberula</i> | Lauraceae | 10 |
| 16 | <i>Ocotea</i> sp. | Lauraceae | 3 |
| 17 | <i>Tetrorchidium rubrivenium</i> | Euphorbiaceae | 1 |
| 18 | <i>Cabralea canjerana</i> | Meliaceae | 3 |
| 19 | <i>Myrsine ferruginea</i> | Myrsinaceae | 3 |
| 20 | <i>Myrsina umbellata</i> | Myrsinaceae | 3 |
| 21 | <i>Clethra scabra</i> | Clethraceae | 2 |
| 22 | <i>Sclerolobium paniculatum</i> | Fabaceae | 2 |
| 23 | <i>Diptychandra aurantiaca</i> | Fabaceae | 1 |
| 24 | <i>Ilex dumosa</i> | Aquifoliaceae | 2 |
| 25 | <i>Cedrela fissilis</i> | Meliaceae | 3 |
| 26 | <i>Montevertedia gonoclada</i> | Celastraceae | 2 |
| 27 | <i>Annona neoinsignis</i> | Annonaceae | 3 |
| 28 | <i>Guatteria australis</i> | Annonaceae | 3 |
| 29 | <i>Joannesia princeps</i> | Euphorbiaceae | 1 |
| 30 | <i>Pseudobombax grandiflorum</i> | Malvaceae | 2 |
| 31 | <i>N.I</i> | | 3 |
| 32 | <i>Aegiphila sellowiana</i> | Lamiaceae | 1 |
| 33 | <i>Nectandra rigida</i> | Lauraceae | 2 |
| 34 | <i>Nectandra</i> sp. | Lauraceae | 2 |
| 35 | <i>Trema micrantha</i> | Cannabaceae | 1 |
| 36 | <i>Psychotria nuda</i> | Rubiaceae | 5 |
| 37 | <i>Campomanesia xanthocarpa</i> | Myrthaceae | 1 |
| 38 | <i>Eugenia</i> spp | Myrthaceae | 5 |
| 39 | <i>Eugenia florida</i> | Myrthaceae | 2 |
| 40 | <i>Eugenia Hiemalis</i> | Myrthaceae | 2 |
| 41 | <i>Eugenia schuechiana</i> | Myrthaceae | 3 |
| 42 | <i>Myrcia neoclusiifolia</i> | Myrthaceae | 3 |
| 43 | <i>Eugenia cerasiflora</i> | Myrthaceae | 1 |
| 44 | <i>Inga fagifolia</i> | Fabaceae | 3 |
| 45 | <i>Tibouchina trichopoda</i> | Melastomataceae | 2 |
| 46 | <i>Sloanea monosperma</i> | Elaeocarpaceae | 3 |
| 47 | <i>Heronima alchorneoides</i> | Phyllanthaceae | 3 |
| 49 | <i>Pimenta pseudocaryophyllus</i> | Myrthaceae | 2 |
| 50 | <i>Bathysa australis</i> | Rubiaceae | 5 |
| 51 | <i>Didymopanax morototoni</i> | Araliaceae | 5 |

(continued on next page)

Table A2 (continued)

| List | Scientific name | Family | No. |
|------|---------------------------------|-----------------|-----|
| 52 | <i>Casearia sylvestris</i> | Flacourtiaceae | 3 |
| 53 | <i>Dendropanax cuneatus</i> | Araliaceae | 3 |
| 54 | <i>Andira fraxinifolia</i> | Fabaceae | 3 |
| 55 | <i>Copaifera trapezifolia</i> | Fabaceae | 3 |
| 56 | <i>Aniba rosaeodora</i> | Lauraceae | 2 |
| 57 | <i>Luehea divaricata</i> | Malvaceae | 2 |
| 58 | <i>Aspidosperma polyneuron</i> | Apocynaceae | 3 |
| 59 | <i>Prunus Sellowii</i> | Rosaceae | 1 |
| 60 | <i>Leandra angustifolia</i> | Melastomataceae | 2 |
| 61 | <i>Miconia organensis</i> | Melastomataceae | 3 |
| 62 | <i>Ocotea odorifera</i> | Lauraceae | 3 |
| 63 | <i>Pera glabrata</i> | Peraceae | 2 |
| 64 | <i>Alchornea triplinervia</i> | Euphorbiaceae | 1 |
| 65 | <i>Alchornea sidifolia</i> | Euphorbiaceae | 4 |
| 66 | <i>Piptocarpha angustifolia</i> | Asteraceae | 2 |
| 67 | <i>Piptocarpha</i> spp | Asteraceae | 15 |

Data availability

Data will be made available on request.

References

Affleck, D.L.R., Diéguez-Aranda, U., 2016. Additive nonlinear biomass equations: a likelihood-based approach. *For. Sci.* 62 (2), 129–140. <https://doi.org/10.5849/forsci.15-126>.

Alvares, C.A., Stape, J.L., Sentelhas, P.C., Gonçalves, J.L.M., Sparovek, G., 2014. Köppen's climate classification map for Brazil. *Meteorol. Z.* 22 (6), 711–728. <https://doi.org/10.1127/0941-2948/2013/0507>.

Andrade, D.V.P., Pasini, F.S., Scarano, F.R., 2020. Syntropy and innovation in agriculture. *Curr. Opin. Environ. Sustain.* 45, 20–24. <https://doi.org/10.1016/j.cosust.2020.08.003>.

Balbinot, R., Trautenmüller, J.W., Caron, B.O., Borella, J., Costa Júnior, S., Breunig, F.M., 2017. Vertical distribution of aboveground biomass in a seasonal deciduous forest. *Revista Brasileira De Ciências Agrárias* 12 (3), 361–365. <https://doi.org/10.5039/agraria.v12i3a5448>.

Balboa-Murias, M.A., Rodríguez-Soalleiro, R., Merino, A., Álvarez-González, J.G., 2006. Temporal Variations and distribution of carbon stocks in aboveground biomass of radiata pine and maritime pine pure stands under different silvicultural alternatives. *For. Ecol. Manage.* 237, 29–38. <https://doi.org/10.1016/j.foreco.2006.09.024>.

Barreto, F.T.C., Curbani, F.E., Zieliński, G.M., Silva, M.B.L., Lacerda, K.C., Rodrigues, D.F., 2023. Development of a multigrid operational forecast system for the oceanic region off Rio de Janeiro State. *Ocean Model.* 184, 102206. <https://doi.org/10.1016/j.ocemod.2023.102206>.

Basuki, T.M., Van Laake, P.E., Skidmore, A.K., Hussin, Y.A., 2009. Allometric equations for estimating the above-ground biomass in tropical lowland *Dipterocarp* forest. *For. Ecol. Manage.* 257, 1684–1694. <https://doi.org/10.1016/j.foreco.2009.01.027>.

Behling, A., Péllico Netto, S., Sanquetta, C.R., Dalla Corte, A.P., Affleck, D.L.R., Rodrigues, A.L., Behling, M., 2018. Critical analyses when modeling tree biomass to ensure additivity of its components. *Annals of the Brazilian Academy of Sciences* 90 (2), 1759–1774. <https://doi.org/10.1590/0001-3765201820170684>.

Bi, H., Long, Y., Turner, J., Lei, Y., Snowdon, P., Li, Y., Harper, R., Zerihun, A., Ximenes, F., 2010. Additive prediction of aboveground biomass for *Pinus radiata* (D. Don) plantations. *For. Ecol. Manage.* 259, 2301–2314. <https://doi.org/10.1016/j.foreco.2010.03.003>.

Blujdea, V.N.B., Pilli, R., Ciuvat, L., Abrudan, I.V., 2012. Allometric biomass equations for young broadleaved trees in plantations in Romania. *For. Ecol. Manage.* 264, 172–184. <https://doi.org/10.1016/j.foreco.2011.09.042>.

Bordin, K.M., Esquivel-Muelbert, A., Bergamin, R.S., Klipel, J., Picolotto, R.C., Frangipani, M.A., Zanini, K.J., Cianciaruso, M.V., Jarenkov, J.A., Jurinat, C.F., Molz, M., Higuchi, P., Silva, A.C., Müller, S.C., 2021. Climate and large-sized trees, but not diversity, drive above-ground biomass in subtropical forests. *For. Ecol. Manage.* 490, 119126. <https://doi.org/10.1016/j.foreco.2021.119126>.

Butler, B.J., Sass, E.M., Gamarra, J.G.P., Campbell, J.L., Wayson, C., Olgún, M., Carrillo, O., Yanai, R.D., 2024. Uncertainty in REDD+ carbon accounting: a survey of experts involved in REDD+ reporting. *Carbon Balance Manag.* 19, 22. <https://doi.org/10.1186/s13021-024-00267-z>.

Carroll, R.J., Ruppert, D., 1988. Transformation and weighting in regression. Chapman & Hall, New York, p. 249.

Chave, J., Réjou-Méchain, M., Bürquez, A., Chidumayo, E., Colgan, M.S., Delitti, W.B.C., Duque, A., Eid, T., Fearsides, P.M., Goodman, R.C., Henry, M., Martínez-Yrízar, A., Mugasha, W.A., Muller-Landau, H.C., Mencuccini, M., Nelson, B.W., Ngomanda, A., Nogueira, E.M., Ortiz-Malavassi, E., Pélassier, R., Ploton, P., Ryan, C.M., Saldarriaga, J.G., Vieilledent, G., 2014. Improved allometric models to estimate the aboveground biomass of tropical trees. *Glob. Chang. Biol.* <https://doi.org/10.1111/gcb.12629>.

Chiyenda, S.S., Kozak, A., 1984. Additivity of component biomass regression equations when the underlying model is linear. *Can J for Res.* 14, 441–446.

Cook-Patton, S.C., Drever, C.R., Griscom, B.W., Hamrick, K., Hardman, H., Kroeger, T., Pacheco, P., Raghav, S., Stevenson, M., Webb, C., Yeo, S., Ellis, P.W., 2021. Protect, manage and then restore lands for climate mitigation. *Nat. Clim. Chang.* 11, 1027–1034. <https://doi.org/10.1038/s41558-021-01198-0>.

Cunia, T., Briggs, R.D., 1984. Forcing additivity of biomass tables—some empirical results. *Can. J. For. Res.* 14, 376–384.

Daiglou, V., Doelman, J., Wicke, B., Faaij, A., Vuuren, D., 2019. Integrated assessment of biomass supply and demand in climate change mitigation scenarios. *Glob. Environ. Chang.* 54, 88–101. <https://doi.org/10.1016/j.gloenvcha.2018.11.012>.

David, A.C., Barbosa, R.I., Vibrans, A.C., Watzlawick, L.F., Trauttmüller, J.W., Balbinot, R., Ribeiro, S.C., Jacovine, L.A.G., Dalla Corte, A.P., Sanquetta, C.R., Silva, A.C., Freitas, J.V., MacFarlane, D.W., 2022. The tropical biomass & carbon project—An application for forest biomass and carbon estimates. *Ecol. Model.* 472 (110067), 2022. <https://doi.org/10.1016/j.ecolmodel.2022.110067>.

Di Corpo, U., Vannini, A., 2014. Syntropy and Sustainability. *Proceedings of the 58th Annual Meeting of the ISSS - 2014 United States*, 1(1). Retrieved from <https://journals.issss.org/index.php/proceedings58th/article/view/2176>.

Erb, K., Kastner, T., Plutzar, C., Bais, A., Carvalhais, N., Petzel, T., Gingrich, S., Haberl, H., Lauk, C., Niedertscheider, M., Pongratz, J., Thurner, M., Luyssaert, S., 2017. Unexpectedly large impact of forest management and grazing on global vegetation biomass. *Nature* 553, 73–76. <https://doi.org/10.1038/nature25138>.

Ferreira, M.I., 2024. Extreme rain event highlights the lack of governance to face climate change in the Southeastern coast of Brazil. *Geogr. Sustainability* 5, 29–32. <https://doi.org/10.1016/j.geosus.2023.11.001>.

Goodman, R.C., Phillips, O.L., Baker, T.R., 2014. The importance of crown dimensions to improve tropical tree biomass estimates. *Ecol. Appl.* 24, 680–698. <https://doi.org/10.1890/13-0070.1>.

Freund, J., Pauly, M., Gochberg, W., Dangremont, E.M., Korchinsky, M., 2024. A novel deforestation risk and baseline allocation model for the next generation of nested REDD+ projects. *Sci. Rep.* 14, 15138. <https://doi.org/10.1038/s41598-024-65141-x>.

Greene, W.H., 2012. *Econometric analysis*. Seventh Edition, Pearson, p. 1238p.

Griscom, B., Shoch, D., Stanley, B., Cortez, R., Virgilio, N., 2009. Sensitivity of amounts and distribution of tropical forest carbon credits depending on baseline rules. *Environ. Sci. Policy* 12 (7), 897–911. <https://doi.org/10.1016/j.envsci.2009.07.008>.

Gujarati, D.N., Porter, D.C., 2009. *Basic Econometrics*, 5. ed. McGraw-Hill, Boston, p. 922p.

Harvey, A.C., 1976. Estimating regression models with multiplicative heteroscedasticity. *Econometrica* 44, 461–465. <https://doi.org/10.2307/1913974>.

Hausemer, G., 2008. *About. Multicultural Luxembourg*, 20.

IBGE - Instituto Brasileiro de Geografia e Estatística, 2012. *Manual Técnico da Vegetação Brasileira*, 2 eds, p. 271. Rio de Janeiro.

IPCC – Intergovernmental Panel on Climate Change, 2006. *Guidelines for National Greenhouse Gas Inventories, Prepared by the National Greenhouse Gas Inventories Programme*. IGES, Japão.

IPCC - Climate Change 2021, 2021. The Physical Science Basis. Contribution of Working Group I to the Sixth Assessment Report of the Intergovernmental Panel on Climate Change. Technical report, IPCC. Mason-Delmotte V, Zhai P, Pirani A, Connors SL, Pean C, Berger S, Caud N, Chen Y, Goldfarb L, Gomis MI, Huang M, Leitzell K, Lonnoy E, Matthews JBR, Maycock TK, Waterfield T, Yelekci O, Yu R, Zhou B (eds.) <https://www.ipcc.ch/report/ar6/wg1/>.

Jacobs, M.W., Cunia, T., 1980. Use of dummy variables to harmonize tree biomass tables. *Can. J. For. Res.* 10, 483–490. <https://doi.org/10.1139/x80-079>.

Jiang, F., Sun, H., Ma, K., Fu, L., Tang, J., 2022. Improving aboveground biomass estimation of natural forests on the Tibetan Plateau using spaceborne LiDAR and machine learning algorithms. *Ecol. Ind.* 143, 109365. <https://doi.org/10.1016/j.ecolind.2022.109365>.

Kozak, A., 1970. Methods of ensuring additivity of biomass components by regression analysis. *For. Chron.* 46 (5), 402–404. <https://doi.org/10.5558/tfc46402-5>.

Lima, R.B., Alves Júnior, F.T., Oliveira, C.P., Silva, J.A.A., Ferreira, R.L.C., 2017. Predicting of biomass in Brazilian tropical dry forest: a statistical evaluation of generic equations. Annals of the Brazilian Academy of Sciences 89 (3), 1815–1828. <https://doi.org/10.1590/0001-3765201720170047>.

Lindenmayer, D.B., Laurance, W.F., Franklin, J.F., 2012. Global Decline in Large Old Trees Science 338, 1305–1306. <https://www.science.org/doi/10.1126/science.1231070>.

Lutz, J.A., Furniss, T.J., Johnson, D.J., Davies, S.J., Allen, D., Alonso, A., et al., 2018. Global importance of large-diameter trees. Glob. Ecol. Biogeogr. 27, 849–864. <https://doi.org/10.1111/geb.12747>.

Ma, Z., Liu, H., Mi, Z., Zhang, Z., Wang, Y., Xu, W., Jiang, L., He, J., 2017. Climate warming reduces the temporal stability of plant community biomass production. Nat. Commun. 8. <https://doi.org/10.1038/ncomms15378>.

Maschler, J., Bialic-Murphy, L., Wan, J., Andresen, L., Zohner, C., Reich, P., Lüscher, A., Schneider, M., Müller, C., Moser, G., Dukes, J., Schmidt, I., Bilton, M., Zhu, K., Crowther, T., 2022. Links across ecological scales: Plant biomass responses to elevated CO₂. Glob. Chang. Biol. 28, 6115–6134. <https://doi.org/10.1111/gcb.16351>.

Myers, N., Mittermeier, R.A., Mittermeier, C.G., Fonseca, G.A.B., Kent, J., 2000. Biodiversity hotspots for conservation priorities. Nature 403, 853–858. <https://doi.org/10.1038/35002501>.

Oliveira, N., Rodríguez-Soalleiro, R., Hernández, M.J., Cañellas, I., Sixto, H., Pérez-Cruzado, C., 2017. Improving biomass estimation in a *Populus* short rotation coppice plantation. For. Ecol. Manage. 391, 194–206. <https://doi.org/10.1016/j.foreco.2017.02.020>.

Pan, Y., Birdsey, R.A., Phillips, O.L., Jackson, R.B., 2013. The Structure, Distribution, and Biomass of the World's Forests. Annu. Rev. Ecol. Evol. Syst. 44 (1), 593–622. <https://doi.org/10.1146/annurev-ecolys-110512-135914>.

Parresol, B.R., 2001. Additivity of nonlinear biomass equations. Can. J. For. Res. 31, 865–878.

Parresol, B.R., 1999. Assessing tree and stand biomass: a review with examples and critical comparisons. For. Sci. 45, 573–593.

Péllico Netto, S., Brena, D.A., 1997. Inventário Florestal. Curitiba, Edição Autores, p. 316p.

Péllico Netto, S., Amaral, M.K., Coraiola, M., 2015. A new index for assessing the value of importance of species – VIS. Annals of the Brazilian Academy of Sciences 87 (4), 2265–2279. <https://doi.org/10.1590/0001-3765201520140351>.

Picard, N., Saint-André, L., Henry, M., 2012. Manual for building tree volume and biomass allometric equations: from field measurement to prediction. In: Rome e Montpellier: Food and Agricultural Organization of the United Nations and Centre De Coopération Internationale En Recherche Agronomique Pour Le Développement, p. 215p.

R Core Team, 2024. R: A Language and Environment for Statistical Computing. R Foundation for Statistical Computing, Vienna, Austria <https://www.R-project.org/>.

Reed, D.D., Green, E.J., 1985. A method of forcing additivity of biomass tables when using nonlinear models. Can. J. For. Res. 15, 1184–1187. <https://doi.org/10.1139/x85-19>.

Romero, F.M.B., Jacobine, L.A.G., Torres, C.M.M.E., Ribeiro, S.C., Rocha, S.J.S.S., Novais, T.N.O., Gaspar, R.O., Silva, L.F., Vidal, E., Leite, H.G., Staudhammer, C.L., Fearnside, P.M., 2022. Aboveground biomass allometric models for large trees in southwestern Amazonia. Trees, Forests and People 9, 100317. <https://doi.org/10.1016/j.tfp.2022.100317>.

Sanquetta, C.R., Behling, A., Dalla Corte, A.P., Péllico Netto, S., Schikowski, A.B., Amaral, M.K., 2015. Simultaneous estimation as alternative to independent modeling of tree biomass. Ann. For. Sci. 72, 1099–1112. <https://doi.org/10.1007/s13595-015-0506-5>.

Santangelo, M., Althuwaynee, O., Alvioli, M., Ardizzone, F., Bianchi, C., Bornaetxea, T., Brunetti, M.T., Bucci, F., Cardinali, M., Donnini, M., Esposito, G., Gariano, S.L., Grita, S., Marchesini, I., Melillo, M., Peruccacci, S., Salvati, P., Yazdani, M., Fiorucci, F., 2023. Inventory of landslides triggered by an extreme rainfall event in Marche-Umbria, Italy, on 15 September 2022. Sci. Data 10 (1), 427.

SAS Institute Inc., 2012. SAS® OnDemand for Academics: Student User's Guide, Second Edition. Cary, NC: SAS Institute Inc.

SEAS – Secretaria do Estado do Ambiente e Sustentabilidade, 2019. Rio de Janeiro State Appendix, 8p. <https://www.theclimategroup.org/sites/default/files/2020-10/Rio%20de%20Janeiro%20Appendix%202019.pdf>.

SFB - SERVIÇO FLORESTAL BRASILEIRO, 2018a. Inventário Florestal Nacional: principais resultados: Paraná. Brasília, DF: MMA, 84 p. (Série Relatórios Técnicos - IFN). <https://coalizaobr.com.br/phocadownload/biblioteca/Inventario-Florestal-Nacional-do-SFB-Parana.pdf>.

SFB - SERVIÇO FLORESTAL BRASILEIRO, 2018b. Inventário Florestal Nacional: principais resultados: Santa Catarina. Brasília, DF: MMA, 106 p. (Série Relatórios Técnicos - IFN). https://acr.org.br/wp-content/uploads/2022/01/31-Relatorio_Tecnico_Inventario_Florestal_Nacional_SC_2018.pdf.

Schumacher, F.X., Hall, F.S., 1933. Logarithmic expression of timber-tree volume. J. Agric. Res. 47 (9), 719–734.

Sileshi, G.W., 2014. A critical review of forest biomass estimation models, common mistakes and corrective measures. For. Ecol. Manage. 329, 237–254. <https://doi.org/10.1016/j.foreco.2014.06.026>.

Spurr, S.H., 1952. Forest inventory. The Ronald Press Company, New York, p. 476.

Tao, K., Fang, J., Yang, W., Fang, J., Liu, B., 2023. Characterizing compound floods from heavy rainfall and upstream–downstream extreme flow in middle Yangtze River from 1980 to 2020. Nat. Hazards 115 (2), 1097–1114. <https://doi.org/10.1007/s11069-022-05585-4>.

Timilsina, N., Beck, J.L., Eames, M.S., Hauer, R., Werner, L., 2017. A comparison of local and general models of leaf area and biomass of urban trees in USA. Urban For. Urban Green. 24, 157–163. <https://doi.org/10.1016/j.ufug.2017.04.003>.

Tradowsky, J.S., Philip, S.Y., Kreienkamp, F., Kew, S.F., Lorenz, P., Arrighi, J., Bettmann, T., Caluwaerts, S., Chan, S.C., De Cruz, L., de Vries, H., Demuth, N., Ferrone, A., Fischer, E.M., Fowler, H.J., Goergen, K., Heinrich, D., Henrichs, Y., Kaspar, F., Lenderink, G., Nilson, E., Otto, F.E.L., Ragone, F., Seneviratne, S.I., Singh, R.K., Skålevåg, A., Termonia, P., Thalheimer, L., van Aalst, M., Van den Bergh, J., Van de Vyver, H., Vannitsem, S., van Oldenborgh, G.J., Van Schaeybroeck, B., Vautard, R., Vonk, D., Wanders, N., 2023. Attribution of the heavy rainfall events leading to severe flooding in Western Europe during July 2021. Clim. Change 176 (7), 90. <https://doi.org/10.1007/s10584-023-03502-7>.

Trautenmüller, J.W., Péllico Netto, S., Balbinot, R., Watzlawick, L.F., Dalla Corte, A.P., Sanquetta, C.R., Behling, A., 2021. Regression estimators for aboveground biomass and its constituent parts of trees in native southern Brazilian forests. Ecol. Ind. 130, 108025. <https://doi.org/10.1016/j.ecolind.2021.108025>.

Trautenmüller, J.W., Péllico Netto, S., Balbinot, R., David, H.C., Dalla Corte, A.P., Watzlawick, L.F., Sanquetta, C.R., Mallmann, A.A., Engel, K., Behling, A., 2023. Ratio estimators for aboveground biomass and its parts in subtropical forests of Brazil. Ecol. Ind. 154, 110530. <https://doi.org/10.1016/j.ecolind.2023.110530>.

Wang, X., Zhao, D., Liu, G., Yang, C., Teskey, R.O., 2018. Additive tree biomass equations for *Betula platyphylla* Suk. plantations in Northeast China. Ann. For. Sci. 75, 60. <https://doi.org/10.1007/s13595-018-0738-2>.

White, H., 1980. A heteroskedasticity-consistent covariance matrix estimator and a direct test of heteroskedasticity. Econometrica 48, 817–838. <https://www.jstor.org/stable/1912934>.

Zeng, W.S., Zhang, H.R., Tang, S.Z., 2011. Using the dummy variable model approach to construct compatible single-tree biomass equations at different scales – a case study for masson pine (*Pinus massoniana*) in southern China. Can. J. For. Res. 41, 1547–1554. <https://doi.org/10.1139/x11-068>.

Zhao, D., Lynch, T.B., Westfall, J., Coulston, J., Kane, M., Adams, D.E., 2019. Compatibility, development, and estimation of taper and volume equation systems. For. Sci. 65 (1), 1–13. <https://doi.org/10.1093/forsci/fxy036>.

Zhao, D., Kane, M., Markewitz, D., Teskey, R., Clutter, M., 2015. Additive tree biomass equations for midrotation loblolly pine plantations. For. Sci. 61 (4), 316–623. <https://doi.org/10.5849/forsci.14-193>.

Zhou, L., Hong, Y., Li, C., Lu, C., He, Y., Shao, J., Sun, X., Wang, C., Liu, R., Liu, H., Zhou, G., Zhou, X., 2020. Responses of biomass allocation to multi-factor global change: A global synthesis. Agr Ecosyst Environ 304, 107115. <https://doi.org/10.1016/j.agee.2020.107115>.